



Title	Trifurcation of the reaction pathway
Author(s)	Harabuchi, Yu; Nakayama, Akira; Taketsugu, Tetsuya
Citation	Computational and Theoretical Chemistry, 1000, 70-74 https://doi.org/10.1016/j.comptc.2012.09.024
Issue Date	2012-11-15
Doc URL	http://hdl.handle.net/2115/51383
Type	article (author version)
File Information	CTC1000_70-74.pdf



[Instructions for use](#)

Trifurcation of the Reaction Pathway

Yu Harabuchi, Akira Nakayama, and Tetsuya Taketsugu

Department of Chemistry, Faculty of Science, Hokkaido University, Sapporo 060-0810, Japan

ABSTRACT

A concept of *trifurcation of a reaction pathway* is introduced to analyze the case where a downhill path from the first-order saddle point accompanies three branches via the valley-ridge inflection region, leading to three different product minima on the potential energy surface. We provide a detailed analysis on the reaction path for an electron transfer reaction, $\text{HCHO}^- + \text{CH}_3\text{Cl} \rightarrow \text{OH}_2\text{C}-\text{CH}_3^{\cdot\cdot}\text{Cl}^-$, as an illustrative example of the trifurcating reaction path.

1. Introduction

An *intrinsic reaction coordinate* (IRC) has played a significant role in quantum chemical approach to chemical reactions.¹ For an elementary reaction, IRC is defined uniquely as a reaction path which connects two minima (reactant and product) and a first-order saddle point (transition state: TS) on a potential energy surface (PES). In a simple reaction, a potential-energy curvature orthogonal to IRC is always positive along the reaction path and the reaction path proceeds through the valley of the PES, leading to the minimum. Along the IRC, if a potential-energy curvature changes its sign from positive to negative with respect to a transverse vibrational coordinate, geometrical feature changes from valley to ridge, causing the instability of the reaction path.² This feature is called *valley-ridge inflection* (VRI). Valtazanov and Ruedenberg introduced a definition of VRI point as follows: the Hessian matrix has a zero eigenvalue and the corresponding eigenvector is perpendicular to the gradient at that point.³ Since the reaction path tangent vector belongs to a totally-symmetric representation of the molecular point group except at stationary points,⁴ VRI point is found in most cases with respect to a non-totally symmetric coordinate. If ridge character continues to the terminal point of IRC, this terminal is not a minimum but a first-order saddle point which connects two symmetrically equivalent product minima with the lower symmetry. For this type of VRI, there have been a number of theoretical studies, which include the detailed analysis of the PES near IRC,⁵⁻⁸ the second-order Jahn-Teller analysis,⁹ a formulation of the bifurcating reaction path,¹⁰ an investigation of the isotope effects on the bifurcating reaction path,^{11,12} and applications to organic chemical reactions.¹³ Quantum wavepacket simulations have also been performed for this type of the bifurcating reaction path.^{14,15}

Along the IRC, VRI can also occur with respect to a *totally-symmetric* vibrational coordinate. In a reaction path Hamiltonian, one can define a set of transverse vibrational modes through diagonalization of the projected Hessian matrix in the orthogonal subspace to the reaction path tangent vector along the IRC.¹⁶ If the potential curvature along a transverse vibrational coordinate changes its sign from positive to negative along the IRC, geometrical feature of the potential changes from valley to ridge with respect to the corresponding transverse coordinate. Since only the totally-symmetric vibrational modes can have a curvature coupling with the reaction path tangent vector, projecting-out of the reaction path tangent from the Hessian matrix can affect only those totally-symmetric vibrational modes. Therefore, VRI with respect to a non-totally symmetric coordinate exactly indicates appearance of a VRI point on the IRC, while VRI with respect to a totally-symmetric

coordinate does not always indicate appearance of a VRI point. Quapp and coworkers^{17,18} have reported deep discussions on the VRI points and valley-ridge border lines on a global potential energy surface.

Appearance of VRI with respect to a totally-symmetric vibrational coordinate along the IRC suggests the possibility of existence of product minimum which is different from the terminal of the IRC.¹⁹⁻²⁵ One example is an electron transfer reaction of $\text{HCHO}^- + \text{CH}_3\text{Cl}$, in which the IRC accompanies VRI and ridge-valley inflection (RVI) in the totally-symmetric coordinate at the spin-unrestricted Hartree-Fock (UHF) level, and the terminal of the IRC from the transition state becomes $\text{OH}_2\text{C}-\text{CH}_3 + \text{Cl}^-$ (the substitution: SUB(C)) or $\text{HCHO} + \text{CH}_3 + \text{Cl}^-$ (the cluster of electron-transfer products: C_{ET}), depending on the computational conditions.^{19,20} Yamataka et al. performed ab initio molecular dynamics simulations for this reaction at the UHF level, and discussed the branching ratio of the products, C_{ET} and SUB(C).²¹ Schlegel and coworkers also performed ab initio molecular dynamics simulations considering the temperature effect on this reaction, and discussed the possibility of the stepwise process, $\text{HCHO}^- + \text{CH}_3\text{Cl} \rightarrow \text{C}_{\text{ET}} \rightarrow \text{SUB}(\text{C})$.^{22,23} For this reaction we recently found that VRI and RVI along the IRC observed at the UHF level disappear at the spin-unrestricted Møller-Plesset second-order perturbation theory (UMP2) level, but VRI appears with respect to totally-symmetric and non-totally symmetric transverse coordinates almost simultaneously in a late region of the IRC.²⁴ We also verified that the terminal of the IRC corresponds to a minimum of $\text{OH}_2\text{C}-\text{CH}_3\cdots\text{Cl}^-$ with C_s symmetry, while there are two different minima of $\text{OH}_2\text{C}-\text{CH}_3\cdots\text{Cl}^-$ with C_1 symmetry.

In this paper we discuss a new concept, *trifurcation of the reaction pathway*, by examining in detail the PES for an electron transfer reaction, $\text{HCHO}^- + \text{CH}_3\text{Cl} \rightarrow \text{OH}_2\text{C}-\text{CH}_3\cdots\text{Cl}^-$, where a downhill path from TS accompanies three branches through a VRI region, leading to three different product minima on the PES. A scheme of trifurcation is shown in **Fig. 1**. We illustrate a case of trifurcation by providing a detailed analysis of the PES orthogonal to IRC for this reaction.

2. Computational details

We previously reported²⁴ IRC calculations for $\text{HCHO}^- + \text{CH}_3\text{Cl} \rightarrow \text{OH}_2\text{C}-\text{CH}_3\cdots\text{Cl}^-$ and the following normal mode analyses along the IRC at the UMP2 level with 6-31+G(d) basis sets. In this paper, starting from the VRI region in the late part of the IRC, we attempt to determine three downhill paths leading to three different product minima of $\text{OH}_2\text{C}-\text{CH}_3\cdots\text{Cl}^-$. A series of potential energy contour plots which are orthogonal to the IRC are also generated to analyze the feature of the PES near VRI region. All calculations were performed using the GAMESS program package.²⁶

3. Results and discussion

First a brief explanation is given for the reaction path of $\text{HCHO}^- + \text{CH}_3\text{Cl}$. In this reaction, electron is transferred from HCHO^- to CH_3Cl , leading to either $\text{OH}_2\text{C}-\text{CH}_3 + \text{Cl}^-$ (SUB(C)) or $\text{HCHO} + \text{CH}_3 + \text{Cl}^-$ (C_{ET}), via the transition state, ET-TS.^{19,20} At the UMP2/6-31+G(d) level, HCHO^- approaches CH_3Cl with anti-conformation, keeping C_s symmetry throughout, and the IRC is connected from ET-TS to SUB(C) of the C_s symmetry (referred to as SUB(C)- C_s), which is a loosely-bound $\text{OH}_2\text{C}-\text{CH}_3\cdots\text{Cl}^-$ complex and corresponds to a minimum on PES.²⁴ As to a $\text{OH}_2\text{C}-\text{CH}_3\cdots\text{Cl}^-$ complex, right-handed and left-handed minimum-energy structures with C_1 symmetry (referred to as SUB(C)- $\text{C}_1(\text{R})$ and SUB(C)- $\text{C}_1(\text{L})$) are also located, and they are more stable in energy than SUB(C)- C_s by 1.2 kcal/mol.²⁴ The structural difference between SUB(C)- C_s and SUB(C)- $\text{C}_1(\text{R})$ (or SUB(C)- $\text{C}_1(\text{L})$) is simply the position of the Cl^- atom relative to $\text{OH}_2\text{C}-\text{CH}_3$. **Figure 2** shows a scheme of the reaction which contains reactant minimum and expected product minima via ET-TS. We discuss the concept of trifurcation by examining the reaction pathways from ET-TS, where the three product minima (SUB(C)- C_s , SUB(C)- $\text{C}_1(\text{R})$, and SUB(C)- $\text{C}_1(\text{L})$) could be connected through downhill paths.

For this purpose, geometric feature of the PES orthogonal to the IRC is examined. **Figure 3** shows variations of the lowest frequencies for the non-totally-symmetric (denoted as \mathbf{L}_1) and totally-symmetric (denoted as \mathbf{L}_2) transverse vibrational modes along the IRC from ET-TS to SUB(C)- C_s ($s = 0 \sim 15$ bohr $\text{amu}^{1/2}$).²⁴ It is noted that \mathbf{L}_2 is derived by the projection technique¹⁶ so as to be orthogonal to the reaction-path tangent vector in which HCHOCH_3 and Cl^- depart from each other. As shown in Fig. 3, the \mathbf{L}_1 and \mathbf{L}_2 modes exhibit imaginary frequencies at $s = 5.82$ and 5.94 bohr $\text{amu}^{1/2}$, respectively, indicating almost simultaneous appearance of VRI in the non-totally symmetric coordinate and in the totally-symmetric coordinate around these regions. The \mathbf{L}_1 and \mathbf{L}_2 modes at $s = 6.0$ bohr $\text{amu}^{1/2}$ are also shown in Fig. 3, where both modes correspond to rotational modes of HCHOCH_3 relative to Cl^- . The appearance of the non-totally symmetric VRI point can be explained by the vibronic interaction between the electronic ground and excited states; the non-totally-symmetric excited state can mix with the totally symmetric ground state through geometrical deformation in a normal coordinate of the non-totally-symmetric representation when these two electronic states come close to each other, as indicated by the second-order Jahn-Teller theory.⁹ This vibronic interaction can invoke change of geometrical feature of the PES from valley to ridge. **Figure 4** shows variations of the ground-state ($1^2\text{A}'$) and

excited-state ($1^2A''$) potential energies along the IRC calculated by the UMP2/6-31+G(d) method,²⁴ where energy values are relative to a sum of energies of reactants, HCHO^- and CH_3Cl . As clearly shown here, the excited state approaches rapidly the ground state at $s = 5.8 \text{ bohr amu}^{1/2}$ and invokes non-totally symmetric VRI on the IRC around this region.

The appearance of VRI along the IRC is a sign that the reaction path is unstable, and new bifurcating paths can be generated, each of which can lead to a different product minimum. In order to gain insight to this mechanism, PES around the VRI region is examined. Since VRI occurs in the two modes (\mathbf{L}_1 and \mathbf{L}_2) almost simultaneously, a series of two-dimensional PESs in these modes are generated at a selected points on the IRC ($s = 5.5, 6.0, 8.5,$ and $11.5 \text{ bohr amu}^{1/2}$). Each of the two-dimensional PES is spanned by the normal coordinates of \mathbf{L}_1 and \mathbf{L}_2 , which are defined as Q_1 (A'') and Q_2 (A'), respectively. The contour plots are given in **Fig. 5**. When the IRC goes through the valley on the PES, the origin of the two-dimensional PES corresponds to a minimum as shown in Fig. 5a ($s = 5.5$). After passing through non-totally-symmetric ($s = 5.82$) and totally-symmetric ($s = 5.94$) VRI region, the origin becomes second-order saddle point (SOSP), and two minima and two first-order saddle points (FOSPs) are located around the origin, as indicated in Fig. 5b ($s = 6.0$). At $s = 8.5$, a potential curvature of the totally-symmetric mode (\mathbf{L}_2) exhibits a real frequency, which indicates that the valley character is recovered for \mathbf{L}_2 at this point (through the ridge-valley inflection (RVI)), while the non-totally-symmetric mode (\mathbf{L}_1) still possesses ridge character. Therefore the origin in the plot becomes FOSP and two minima are located in the Q_1 direction (See Fig. 5c). These two minima observed at $s = 6.0$ and 8.5 will be linked to $\text{SUB(C)-C}_1(\text{R})$ and $\text{SUB(C)-C}_1(\text{L})$, as shown below. At $s = 10.5$, the non-totally-symmetric mode (\mathbf{L}_1) also exhibits valley character through RVI and the origin of the PES again corresponds to the minimum, which leads to the product minimum of SUB(C)-C_s as a terminal of IRC.

As seen above, there are three product minima (SUB(C)-C_s , $\text{SUB(C)-C}_1(\text{R})$, and $\text{SUB(C)-C}_1(\text{L})$) from ET-TS. It is obvious that SUB(C)-C_s is connected by the IRC, while it is a difficult task to determine continuous downhill paths leading to $\text{SUB(C)-C}_1(\text{R})$ or $\text{SUB(C)-C}_1(\text{L})$. Previously Yanai et al.¹⁰ attempted to explore an important region on the PES for bifurcating reactions by calculating a group of steepest descent paths from zero-point vibrational energy region around the VRI point, and found that those steepest descent paths mostly run in parallel with the IRC since negative energy gradients along the IRC are more effective to push molecules than the instability of the IRC. In the present study, we attempted to determine continuous downhill paths from the VRI point to $\text{SUB(C)-C}_1(\text{R})$ (or

SUB(C)-C₁(L)) by deviating molecular coordinates in the Q_1 (A'') direction slightly and calculating steepest descent paths, but they all reached SUB(C)-C_s minimum. After several attempts, we finally succeeded to obtain the downhill paths to SUB(C)-C₁(R) minimum; first a linearly-interpolated path is defined between the point around the VRI region (at $s = 6.0$) and the points determined by moving Cl⁻ in a combination of Q_1 (A'') and Q_2 (A'), and then a steepest-descent-path is calculated from the latter point. **Figure 6** shows a variation of the energy (a) along the steepest descent path from ET-TS to SUB(C)-C_s and (b) along the newly-determined path from ET-TS to SUB(C)-C₁(R) (or SUB(C)-C₁(L)) where cross mark (×) and round mark (○) denote the linearly-interpolated path ($s = 6.0 \sim 16.8$ bohr amu^{1/2}) and the steepest descent path ($s = 16.8 \sim 38.7$ bohr amu^{1/2}), respectively. In the latter path, Cl⁻ initially goes toward the direction of a combination of Q_1 (A'') and Q_2 (A'), and then it moves around CH₃CHO and reaches its position at SUB(C)-C₁(R).

As examined here, we demonstrate that it is possible to define downhill paths starting from the single TS to the three product minima, SUB(C)-C_s, SUB(C)-C₁(R), and SUB(C)-C₁(L), *via* the VRI region, and this can be regarded as a case of trifurcation of the reaction path. Here we should comment on the geometrical feature around the VRI region. In this reaction, VRI occurs for two modes almost simultaneously (non-totally-symmetric and totally-symmetric directions) and the two minima are located in the two-dimensional PES spanned by the normal coordinates of the corresponding modes. These two minima are successfully connected to the different product minima. In the other type of reactions where the VRI occurs simultaneously for multiple modes, there is the possibility that more than two minima are located in the PES spanned by the normal coordinates of the imaginary frequency modes and these minima could be connected to the different product minima. In this case, although it would be highly rare, more branching path than trifurcation could be generated. As explored in the present work, the analysis based on the PES spanned by the normal coordinates of imaginary frequency modes provides a useful information on the multi-branching reactions.

4. Concluding remarks

In this paper, a concept, *trifurcation of the reaction pathway*, is introduced and discussed by examining the IRC for an electron transfer reaction, $\text{HCHO}^- + \text{CH}_3\text{Cl} \rightarrow \text{OH}_2\text{C}-\text{CH}_3\cdots\text{Cl}^-$. It is demonstrated that it is possible to define downhill paths starting from a single TS to three different product minima, and this case is considered as the trifurcation of the reaction pathway since the reaction path splits to three branches at the VRI region. We provide a detailed analysis of the mechanism of trifurcation by examining successive two-dimensional PESs around the VRI region spanned by the normal coordinates of the imaginary frequency modes. This type of analyses will help to understand reaction mechanism for a case of multi-branching reaction pathways.

Acknowledgments

This work was supported by a Grant-in-Aid for Scientific Research from the Ministry of Education, Culture, Sports, Science and Technology. The computations were performed using the Research Center for Computational Science, Okazaki, Japan. Y. H. thanks the Japan Society for the Promotion of Science for Research Fellowships for Young Scientists.

References

- [1] K. Fukui, A formulation of the reaction coordinate, *J. Phys. Chem.* 74 (1970) 4161-4163.
- [2] A. Tachibana, I. Okazaki, M. Koizumi, K. Hori, and T. Yamabe, Stability of the reaction coordinate in the unimolecular reaction of thioformaldehyde, *J. Am. Chem. Soc.* 107 (1985) 1190-1196.
- [3] P. Valtazanos and K. Ruedenberg, Bifurcations and transition states, *Theor. Chim. Acta* 69 (1986) 281-307.
- [4] H. Metiu, J. Ross, R. Silbey, and T. F. George, On symmetry properties of reaction coordinates, *J. Chem. Phys.* 61 (1974) 3200-3209.
- [5] W. Quapp, Gradient extremals and valley floor bifurcations on potential-energy surfaces, *Theor. Chim. Acta* 75 (1989) 447-460.
- [6] H. B. Schlegel, Some thoughts on reaction-path following, *J. Chem. Soc.-Faraday Trans.* 90 (1994) 1569-1574.
- [7] T. Taketsugu, N. Tajima, and K. Hirao, Approaches to bifurcating reaction path, *J. Chem. Phys.* 105 (1996) 1933-1939.
- [8] W. Quapp, How does a reaction path branching take place? A classification of bifurcating events, *J. Mol. Struct.* 695-696 (2004) 95-101.
- [9] T. Taketsugu and T. Hirano, Mechanism of bifurcation along the reaction path: An application in the case of thioformaldehyde, *J. Chem. Phys.* 99 (1993) 9806-9814.
- [10] T. Yanai, T. Taketsugu, and K. Hirao, Theoretical study of bifurcating reaction paths, *J. Chem. Phys.* 107 (1997) 1137-1146.
- [11] Y. Kumeda and T. Taketsugu, Isotope effect on bifurcating reaction path: Valley-ridge inflection point in totally symmetric coordinate, *J. Chem. Phys.* 113 (2000) 477-484.
- [12] T. Taketsugu and Y. Kumeda, An ab initio direct-trajectory study of the kinetic isotope effect on the bifurcating reaction, *J. Chem. Phys.* 114 (2001) 6973-6982.
- [13] D. A. Singleton, C. Hang, M. J. Szymanski, M. P. Meyer, A. G. Leach, K. T. Kuwata, J. S. Chen, A. Greer, C. S. Foote, and K. N. Houk, Mechanism of ene reactions of singlet oxygen. A two-step no-intermediate mechanism, *J. Am. Chem. Soc.* 125 (2003) 1319-1328.
- [14] B. Lasorne, G. Dive, D. Lauvergnat, and M. Desouter-Lecomte, Wave packet dynamics along bifurcating reaction paths, *J. Chem. Phys.* 118 (2003) 5831-5840.
- [15] B. Lasorne, G. Dive, D. Lauvergnat, and M. Desouter-Lecomte, Wave packets in a bifurcating region of an energy landscape: Diels-Alder dimerization of cyclopentadiene, *J. Chem. Phys.* 122 (2005) 184304.

- [16] W. H. Miller, N. C. Handy, and J. E. Adams, Reaction path Hamiltonian for polyatomic molecules, *J. Chem. Phys.* 72 (1980) 99-112.
- [17] W. Quapp and B. Schmidt, An empirical, variational method of approach to unsymmetric valley-ridge inflection points, *Theor. Chem. Acc.* 128 (2011) 47-61.
- [18] W. Quapp, J. M. Bofill, and A. Aguilar-Mogas, Exploration of cyclopropyl radical ring opening to allyl radical by Newton trajectories: importance of valley-ridge inflection points to understand the topography, *Theor. Chem. Acc.* 129 (2011) 803-821.
- [19] G. N. Sastry and S. Shaik, Structured electron transfer transition state. valence bond configuration mixing analysis and ab initio calculations of the reactions of formaldehyde radical anion with methyl chloride, *J. Phys. Chem.* 100 (1996) 12241-12252.
- [20] S. Shaik, D. Danovich, G. N. Sastry, P. Y. Ayala, and H. B. Schlegel, Dissociative electron transfer, substitution, and borderline mechanisms in reactions of ketyl radical anions. Differences and difficulties in their reaction paths, *J. Am. Chem. Soc.* 119 (1997) 9237-9245.
- [21] H. Yamataka, M. Aida, and M. Dupuis, One transition state leading to two product states: ab initio molecular dynamics simulations of the reaction of formaldehyde radical anion and methyl chloride, *Chem. Phys. Lett.* 300 (1999) 583-587.
- [22] J. Li, X. S. Li, S. Shaik, and H. B. Schlegel, Single transition state serves two mechanisms. Ab initio classical trajectory calculations of the substitution-electron transfer branching ratio in $\text{CH}_2\text{O}^{\cdot-} + \text{CH}_3\text{Cl}$, *J. Phys. Chem. A* 108 (2004) 8526-8532.
- [23] J. Li, S. Shaik, and H. B. Schlegel, A single transition state serves two mechanisms. The branching ratio for $\text{CH}_2\text{O}^{\cdot-} + \text{CH}_3\text{Cl}$ on improved potential energy surfaces, *J. Phys. Chem. A* 110 (2006) 2801-2806.
- [24] Y. Harabuchi and T. Taketsugu, A significant role of the totally symmetric valley-ridge inflection point in the bifurcating reaction pathway, *Theor. Chem. Acc.* 130 (2011) 305-315.
- [25] J. M. Ramírez-Anguita, R. Gelabert, À. González-Lafont, M. Moreno, and J. M. Lluch, A variational transition state theory description of periselectivity effects on cycloadditions of ketenes with cyclopentadiene, *Theor. Chem. Acc.* 128 (2011) 569-577.
- [26] M. W. Schmidt, K. K. Baldrige, J. A. Boatz, S. T. Elbert, M. S. Gordon, J. H. Jensen, S. Koseki, N. Matsunaga, K. A. Nguyen, S. J. Su, T. L. Windus, M. Dupuis, and J. A. Montgomery, General atomic and molecular electronic structure system, *J. Comput. Chem.* 14 (1993) 1347-1363.

FIGURE CAPTION

- Fig. 1.** An illustration of reaction path with one product minimum (simple), two product minima (bifurcation), and three product minima (trifurcation).
- Fig. 2.** A schematic reaction profile for $\text{HCHO}^- + \text{CH}_3\text{Cl} \rightarrow \text{OH}_2\text{C}-\text{CH}_3\cdots\text{Cl}^-$.
- Fig. 3.** Variations of lowest frequencies of non-totally-symmetric and totally-symmetric normal modes orthogonal to the IRC (denoted as \mathbf{L}_1 and \mathbf{L}_2 , respectively) along the reaction path for $\text{ET-TS} \rightarrow \text{SUB(C)}-\text{C}_s (\text{OH}_2\text{C}-\text{CH}_3\cdots\text{Cl}^-)$.
- Fig. 4.** Variations of energies of the ground state (${}^2\text{A}'$) and the first-excited state (${}^2\text{A}''$) along the IRC for $\text{ET-TS} \rightarrow \text{SUB(C)}-\text{C}_s (\text{OH}_2\text{C}-\text{CH}_3\cdots\text{Cl}^-)$.
- Fig. 5.** A series of potential-energy contour plots orthogonal to the IRC.
- Fig. 6.** An energy variation along the path from ET-TS to (a) $\text{SUB(C)}-\text{C}_s$ and (b) $\text{SUB(C)}-\text{C}_1(\text{R})$ or $\text{SUB(C)}-\text{C}_1(\text{L})$.

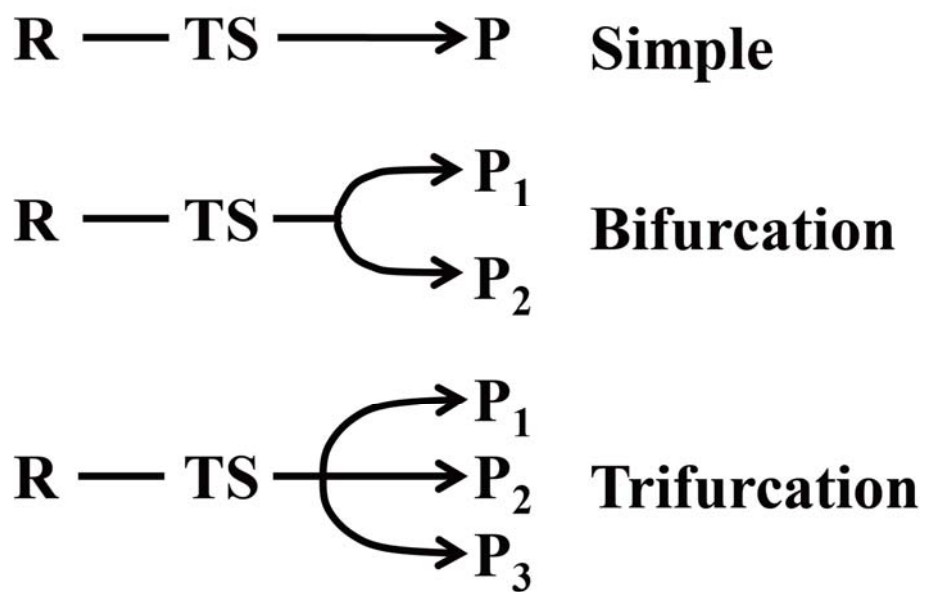


Fig. 1. "Trifurcation of the Reaction Pathway" by Harabuchi et al.

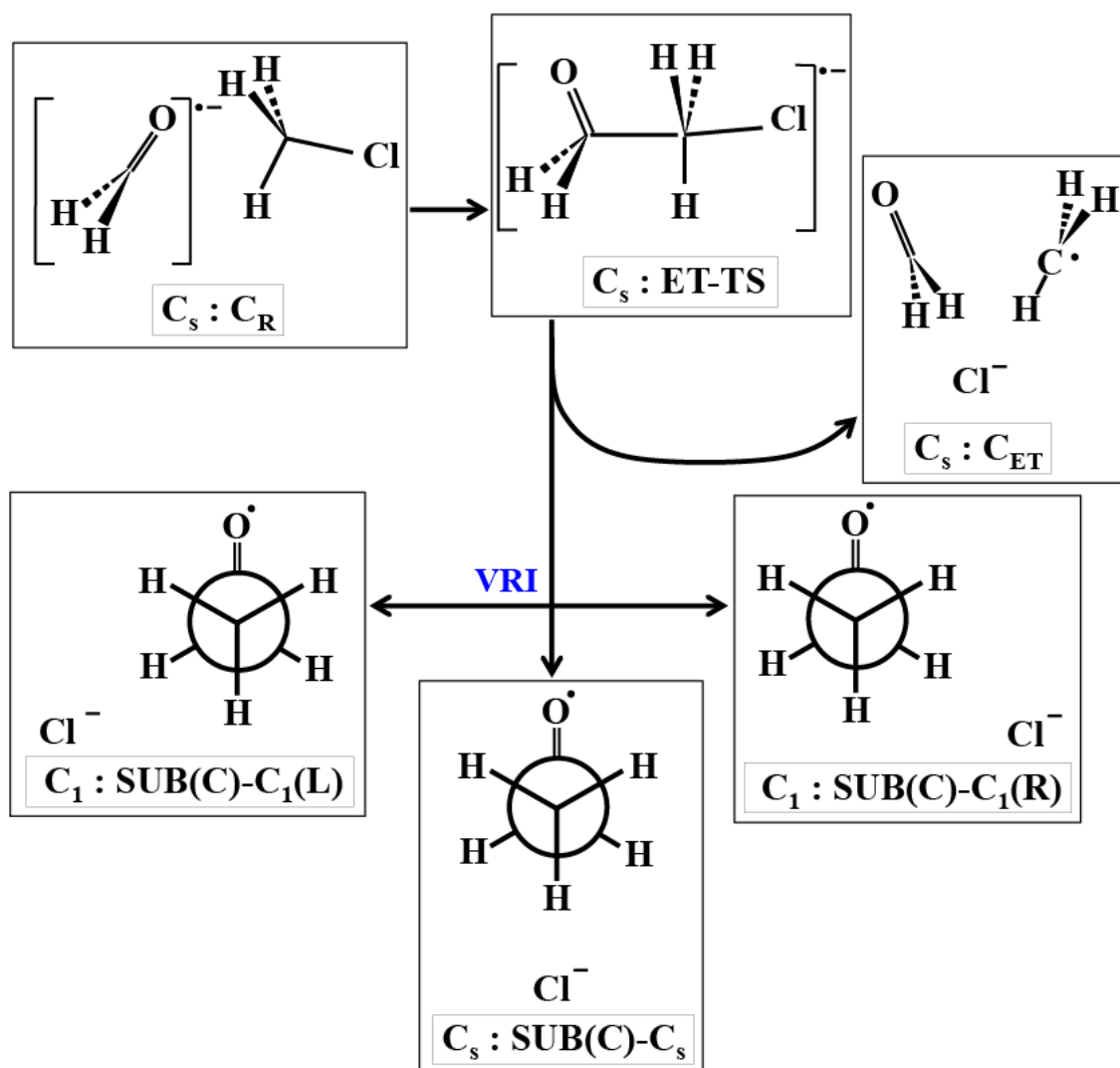


Fig. 2. "Trifurcation of the Reaction Pathway" by Harabuchi et al.

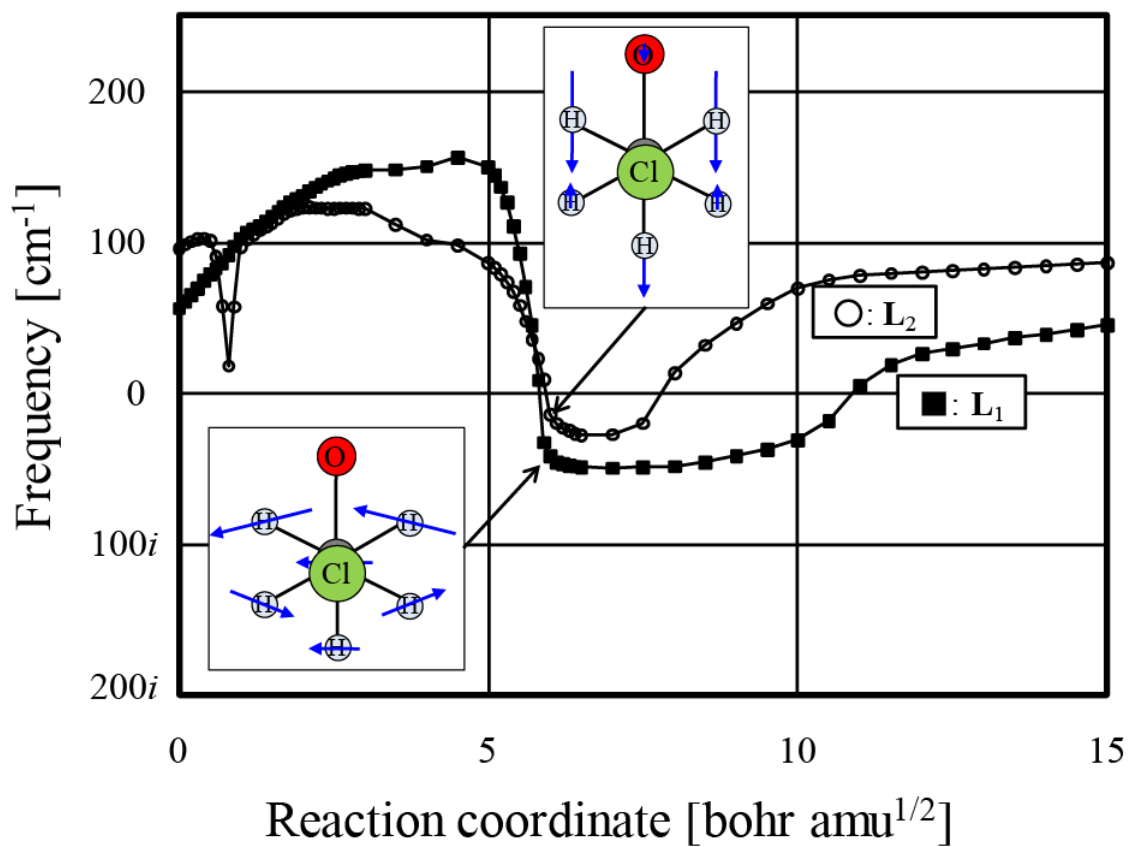


Fig. 3. "Trifurcation of the Reaction Pathway" by Harabuchi et al.

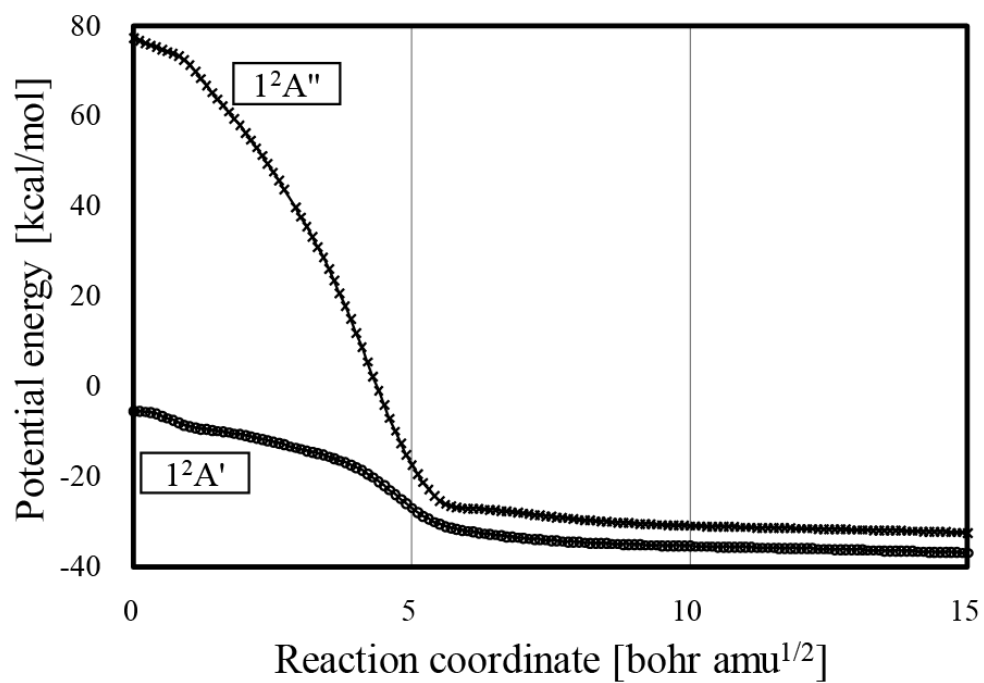


Fig. 4. "Trifurcation of the Reaction Pathway" by Harabuchi et al.

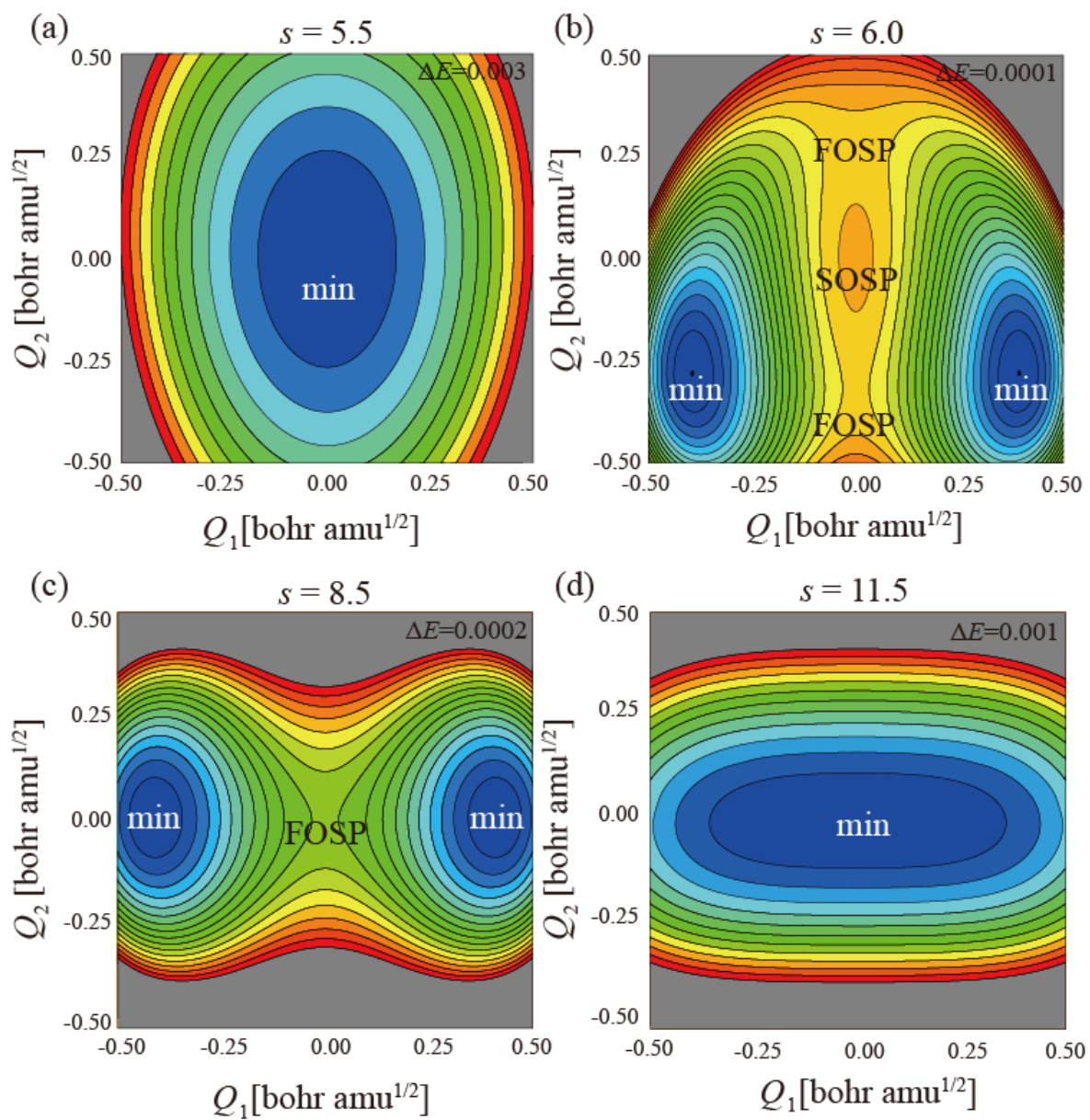


Fig. 5. "Trifurcation of the Reaction Pathway" by Harabuchi et al.

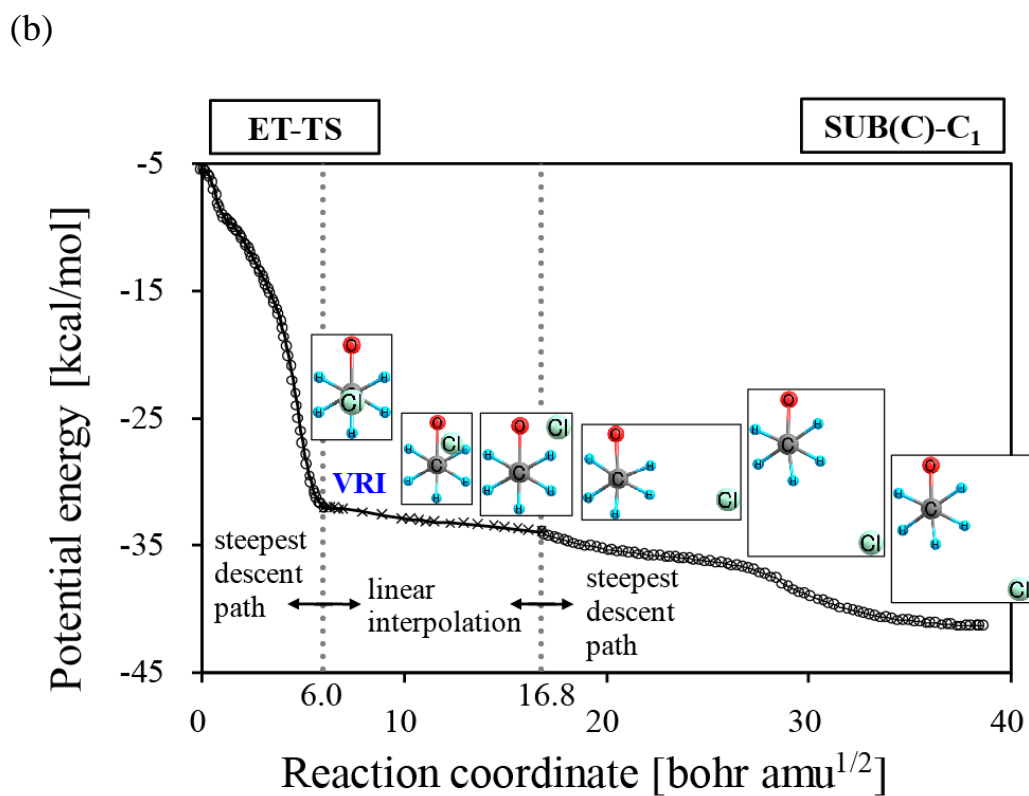
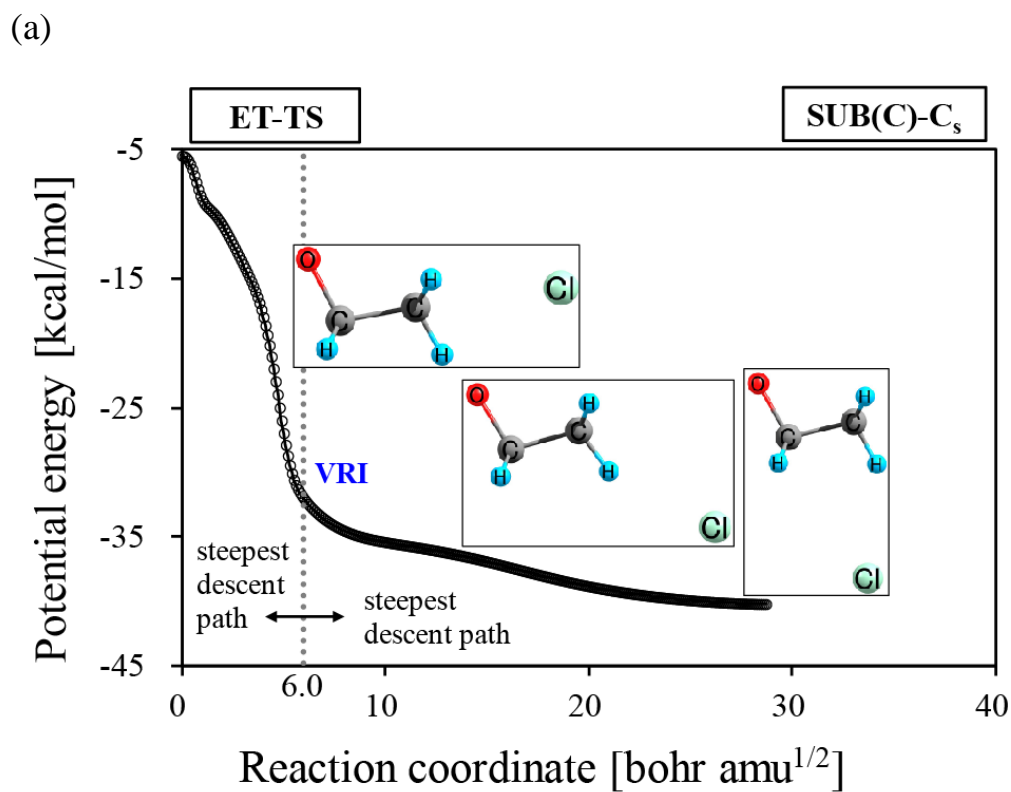


Fig. 6. "Trifurcation of the Reaction Pathway" by Harabuchi et al.